

# Zero-Energy Flows and Vortex Patterns in Quantum Mechanics

Tsunehiro Kobayashi\*

*Department of General Education for the Hearing Impaired, Tsukuba College of Technology  
Ibaraki 305-0005, Japan*

## Abstract

We show that zero-energy flows appear in many particle systems as same as in single particle cases in 2-dimensions. Vortex patterns constructed from the zero-energy flows can be investigated in terms of the eigenstates in conjugate spaces of Gel'fand triplets. Stable patterns are written by the superposition of zero-energy eigenstates. On the other hand vortex creations and annihilations are described by the insertions of unstable eigenstates with complex-energy eigenvalues into the stable patterns. Some concrete examples are presented in the 2-dimensional parabolic potential barrier case. We point out three interesting properties of the zero-energy flows; (i) the absolute economy as for the energy consumption, (ii) the infinite variety of the vortex patterns, and (iii) the absolute stability of the vortex patterns .

Keywords: Zero-energy solutions, vortex creations and annihilations, quantum mechanics, Gel'fand triplets,

---

\*E-mail: kobayash@a.tsukuba-tech.ac.jp

## 1. Introduction

Vortices play interesting roles in various aspects of present-day physics such as vortex matters (vortex lattices) in condensed matters [1, 2], quantum Hall effects [3-5], various vortex patterns of non-neutral plasma [6-9] and Bose-Einstein gases [10-14]. Some fundamental properties and applications of vortices in quantum mechanics were examined by many authors [15-23].

Recently we have proposed a way to investigate vortex patterns in terms of zero-energy solutions of Schrödinger equations in 2-dimensions, which are infinitely degenerate and eigenfunctions in conjugate spaces of Gel'fand triplets (CSGT) [24, 25]. It should be noted that the eigenfunctions in CSGT represent scattering states, and thus they are generally not normalizable [26]. Therefore, the probability density ( $|\psi|^2$ ) and the probability current ( $\mathbf{j} = \text{Re}[\psi^*(-i\hbar\nabla)\psi]/m$ ) for the eigenfunction ( $\psi$ ), which are defined in usual Hilbert spaces, cannot be introduced to the eigenfunctions in CSGT. Instead of the probability current, however, the velocity which is defined by  $\mathbf{v} = \mathbf{j}/|\psi|^2$  can have a well-defined meaning, because the ambiguity due to the normalization of the eigenfunctions disappears in the definition of the velocity. Actually we have shown that many interesting objects used in hydrodynamics such as the complex velocity potential can be introduced in the 2-dimensions of CSGT [27]. We can expect that the hydrodynamical approach is a quite hopeful framework in the investigation of phenomena described in CSGT. One should pay attention to two important facts obtained in the early works [24,25]. One is the fact that the zero-energy solutions are common over the two-dimensional central potentials such that  $V_a(\rho) = -a^2 g_a \rho^{2(a-1)}$  with  $\rho = \sqrt{x^2 + y^2}$  except  $a = 0$  and then similar vortex patterns described by the zero-energy solutions appear in all such potentials. Actually zero-energy solutions for a definite number of  $a$  can be transformed to solutions for arbitrary number of  $a$  by conformal transformations [24, 25]. The other is that the zero-energy solutions are infinitely degenerate, and thus all energy eigenvalues in CSGT with the potentials  $V_a(\rho)$  are infinitely degenerate because the addition of the infinitely degenerate zero-energy solutions to arbitrary eigenfunctions does not change the energy eigenvalues at all.

We, however, have to know that these results are obtained in equations for the single particle. We can, of course, apply the results in scattering processes where injected particles can be treated as individual particles. In the above-mentioned processes where vortices are observed [1-14], however, correlations among constituent particles cannot be ignored. We have to study whether such zero-energy flows appear in many particle systems. Furthermore we also have to study time evolutions of vortex patterns that have already been observed in experiments [6-14]. As for the time evolutions we have to take account of non-zero energy solutions in CSGT. It is known that the non-zero energy solutions generally have complex energy eigenvalues like  $\mathcal{E} = E \mp i\Gamma$  with  $E, \Gamma \in \mathbb{R}$ , and then they have the time developments described by the factors  $e^{-(iE/\hbar \pm \Gamma/\hbar)t}$  [26]. Considering that stationary flows and time-dependent flows are, respectively, represented by the zero-energy solutions and the non-zero energy solutions in CSGT, we can expect that in CSGT

general time-dependent flows are described by linear combinations of the stationary flows written by the zero-energy solutions and non-stationary flows (time-dependent flows) described by non-zero (complex) energy solutions. In hydrodynamics it is well-known that the vortex patterns are important objects to identify the situations of the flows. In the present model we can image two different types of the vortex patterns. One is the stationary vortex patterns, and the other is the vortex patterns varying in the time evolutions. As presented in our early works [24, 25], the stationary vortex patterns can be described by the superposition of the zero-energy solutions, while the time-dependent ones will be done by putting the non-zero energy solutions into the superposition.

In this paper we shall study two problems; one is the zero-energy flows in many particle systems in section 2, and the other is time-developments of vortex patterns in section 3. In order to obtain concrete examples of time-dependent vortex patterns, we shall use the eigenfunctions of the 2-dimensional parabolic potential barrier (2D-PPB) [27] in section 3, because the eigenfunctions with non-zero energy (complex energy) solutions in CSGT are known only in the case of the PPB. It is, however, noticed that the stable vortex patterns obtained in the 2D-PPB can easily be transformed those of the potentials  $V_a(\rho)$  by the conformal transformations [24,25]. From these concrete analyses we shall point out three interesting properties of zero-energy flows in section 4. In section 5 some remarks will be done. Throughout these investigations we shall see that this approach can be one interesting possibility to analyze various time-dependent vortex patterns in a rigorous framework of quantum mechanics in CSGT.

## 2. Zero-energy flows and vortices

### 2.1 Cases of single particle motions

Let us briefly see the arguments for the zero-energy flows in the single particle motions. (For details, see refs. 24 and 25.)

#### (1) Zero-energy flows in single particle motions

In 2-dimensions the eigenvalue problems with the energy eigenvalue  $\mathcal{E}$  are explicitly written by

$$\left[-\frac{\hbar^2}{2m} \Delta + V_a(\rho)\right] \psi(x, y) = \mathcal{E} \psi(x, y), \quad (1)$$

where  $\Delta = \partial^2/\partial x^2 + \partial^2/\partial y^2$ , the central potentials are generally given by  $V_a(\rho) = -a^2 g_a \rho^{2(a-1)}$ , with  $\rho = \sqrt{x^2 + y^2}$ ,  $a \in \mathbb{R}$  ( $a \neq 0$ ), and  $m$  and  $g_a$  are, respectively, the mass of the particle and the coupling constant. Note here that the eigenvalues  $\mathcal{E}$  should generally be complex numbers in CSGT.

Let us consider the conformal mappings  $\zeta_a = z^a$ , with  $z = x + iy$ . We use the notations  $u_a$  and  $v_a$  defined by  $\zeta_a = u_a + iv_a$  that are written as  $u_a = \rho^a \cos a\varphi$ ,  $v_a = \rho^a \sin a\varphi$ , where  $\varphi = \arctan(y/x)$ . In the  $(u_a, v_a)$  plane the equations (1) are written down as

$$a^2 \rho_a^{2(a-1)/a} \left[-\frac{\hbar^2}{2m} \Delta_a - g_a\right] \psi(u_a, v_a) = \mathcal{E} \psi(u_a, v_a), \quad (2)$$

where  $\Delta_a = \partial^2/\partial u_a^2 + \partial^2/\partial v_a^2$ . We see that the equations become same for all values of  $a$  (except  $a = 0$ ) for the energy eigenvalue  $\mathcal{E} = 0$ . In fact, for  $\mathcal{E} = 0$  the equations have the same form as that for the free particle with the constant potentials  $g_a$  as

$$\left[-\frac{\hbar^2}{2m} \Delta_a - g_a\right] \psi(u_a, v_a) = 0. \quad (3)$$

It should be noticed that in the case of  $a = 1$  where the original potential is a constant  $g_1$  the energy does not need to be zero but can take arbitrary real numbers, because the right-hand side of (1) has no  $\rho$  dependence. In the  $a = 1$  case, therefore, we should take  $g_1 + \mathcal{E}$  instead of  $g_a$ . This means that all plane wave solutions have the same infinite degeneracy discussed below.

It is trivial that the equations for all  $a$  have the particular solutions  $\psi_0^\pm(u_a) = N_a e^{\pm i k_a u_a}$  and  $\psi_0^\pm(v_a) = N_a e^{\pm i k_a v_a}$  with  $k_a = \sqrt{2m g_a}/\hbar$  for  $g_a > 0$ . We notice here the degeneracy of the solutions that have already been known in the 2D-PPB [27]. By putting the wave function  $f^\pm(u_a; v_a) \psi_0^\pm(u_a)$  into (3) where  $f^\pm(u_a; v_a)$  is a polynomial function of  $u_a$  and  $v_a$ , we obtain the equation

$$\left[\Delta_a \pm 2i k_a \frac{\partial}{\partial u_a}\right] f^\pm(u_a; v_a) = 0. \quad (4)$$

A few examples of the functions  $f$  are given by

$$\begin{aligned} f_0^\pm(u_a; v_a) &= 1, \\ f_1^\pm(u_a; v_a) &= 4k_a v_a, \\ f_2^\pm(u_a; v_a) &= 4(4k_a^2 v_a^2 + 1 \pm 4ik_a u_a). \end{aligned} \quad (5)$$

We can obtain the general forms of the polynomials in the 2D PPB, which are generally written by the multiple of the polynomials of degree  $n$ ,  $H_n^\pm(\sqrt{2k_2}x)$ , such that  $f_n^\pm(u_2; v_2) = H_n^\pm(\sqrt{2k_2}x) \cdot H_n^\mp(\sqrt{2k_2}y)$ , where  $x$  and  $y$  in the right-hand side should be considered as the functions of  $u_2$  and  $v_2$  [27]. Since the form of the equations (4) is common for all  $a$ , the solutions can be written by the same polynomial functions that are obtained in the PPB. The states expressed by these wave functions belong to the conjugate spaces of Gel'fand triplets of which nuclear space is given by Schwarz space. Actually we easily see that the wave functions cannot be normalized in terms of Dirac's delta functions except the lowest polynomial solutions.

Here it should be stressed that the existence of the infinitely degenerate zero-energy solutions brings the infinite degeneracy to all the eigenstates. This fact means that the energy and the other quantum numbers like angular momentums, which are related to the determination of the energy eigenvalues, are not enough to discriminate the eigenstates. What are good quantum numbers to characterize the infinite degeneracy? An interesting candidate to characterize the states is vortex patterns that tell us topological properties of the states. Note that the vortex patterns have been observed in experiments [8-14]. Time developments of the patterns can also be good observables in those processes.

## (2) Velocity and vortices in quantum mechanics

Let us here briefly note how vortices are interpreted in quantum mechanics. The probability density  $\rho(t, x, y)$  and the probability current  $\mathbf{j}(t, x, y)$  of a wavefunction  $\psi(t, x, y)$  in non-relativistic quantum mechanics are, respectively, defined by  $\rho(t, x, y) \equiv |\psi(t, x, y)|^2$  and  $\mathbf{j}(t, x, y) \equiv \text{Re}[\psi(t, x, y)^* (-i\hbar\nabla) \psi(t, x, y)] / m$ . They satisfy the equation of continuity  $\partial\rho/\partial t + \nabla \cdot \mathbf{j} = 0$ . Following the analogue of the hydrodynamical approach, the fluid can be represented by the density  $\rho$  and the fluid velocity  $\mathbf{v}$ . They satisfy Euler's equation of continuity  $\partial\rho/\partial t + \nabla \cdot (\rho\mathbf{v}) = 0$ . Comparing this equation with the continuity equation, the following definition for the quantum velocity of the state  $\psi(t, x, y)$  is led in the hydrodynamical approach;

$$\mathbf{v} \equiv \frac{\mathbf{j}(t, x, y)}{|\psi(t, x, y)|^2}. \quad (6)$$

Now it is obvious that vortices appear at the zero points of the density, that is, the nodal points of the wavefunction. At the vortices, of course, the current  $\mathbf{j}$  must not vanish. When we write the wavefunction  $\psi(t, x, y) = \sqrt{\rho(x, y)} e^{iS(x, y)/\hbar}$ , the velocity is given by  $\mathbf{v} = \nabla S/m$ . We should here remember that the solutions degenerate infinitely. This fact indicates that we can construct wavefunctions having the nodal points at arbitrary positions in terms of linear combinations of the infinitely degenerate solutions [24, 25, 27].

The strength of vortex is characterized by the circulation  $\Gamma$  that is represented by the integral round a closed contour  $C$  encircling the vortex such that

$$\Gamma = \oint_C \mathbf{v} \cdot d\mathbf{s} \quad (7)$$

and it is quantized as

$$\Gamma = 2\pi l\hbar/m, \quad (8)$$

where the circulation number  $l$  is an integer [16, 18, 20, 23].

## 2.2 Cases of many particle motions

Let us consider a simple system composed of  $N$  number of the same particles with the mass  $m$ .

### (1) Zero-energy flows in many particle cases

The interactions between two constituent particles are supposed to be written by the same potential  $V(\rho_{ij})$ , where  $\rho_{ij} = |\vec{\rho}_i - \vec{\rho}_j|$  stands for the relative distance between two particles. The Schrödinger equation for the  $N$  particle system is written as

$$\left[ -\frac{\hbar^2}{2m} \sum_{i=1}^N \Delta_i + \sum_{i>j}^N \sum_{j=1}^{N-1} V(\rho_{ij}) \right] \Psi(t, \vec{\rho}_1, \dots, \vec{\rho}_N) = \mathcal{E} \Psi(t, \vec{\rho}_1, \dots, \vec{\rho}_N). \quad (9)$$

Introducing a centre of mass coordinate  $\vec{\rho}_C$  and  $N - 1$  relative coordinates  $\vec{\rho}_{r_i}$  with  $i =$

$1, \dots, N-1$ , the equation is rewritten as

$$\left[-\frac{\hbar^2}{2M} \Delta_C - H_r(\rho_{r_1}, \dots, \rho_{r_{N-1}})\right] \Phi_C(t, \vec{\rho}_C) \phi_r(t, \vec{\rho}_{r_1}, \dots, \vec{\rho}_{r_{N-1}}) = \mathcal{E} \Phi_C(t, \vec{\rho}_C) \phi_r(t, \vec{\rho}_{r_1}, \dots, \vec{\rho}_{r_{N-1}}), \quad (10)$$

where  $M = Nm$  and  $H_r(\rho_{r_1}, \dots, \rho_{r_{N-1}})$  stands for the Hamiltonian for the relative coordinates. It should be noted that the centre of mass coordinate can always be separable from the relative ones, and then the energy eigenvalue  $\mathcal{E}$  are written by the sum of the eigenvalue of centre of mass system  $E_C$  and that of the relative ones  $E_r$  as  $\mathcal{E} = E_C + E_r$ . We can consider that the zero-energy solutions can appear in the relative motions, e.g., when the relative interactions are written by the same PPB,  $H_r$  are separable for all the relative coordinates, for which interactions are written by the PPB. Here we shall, however, discuss the case where the flows discussed in the section 2.1 appear in the centre of mass motions, that is, the total flows. Now let us consider the zero-energy solutions of the total system represented by  $\mathcal{E} = 0$ . Considering the equation  $\mathcal{E} = E_C + E_r$ , the flows discussed in the section 2.1 appear for  $E_r < 0$ , because  $E_C > 0$  is required. This means that the relative interactions have to be totally described by a kind of attractive potential. In this case the centre of mass motions  $\Phi_C(t, \vec{\rho}_C)$  are described by the plane waves with the infinite degeneracy, which are obtained from the solutions in the section 2.1 by putting  $a = 1$ . If the Hamiltonian  $H_r$  has levels with different negative-energy eigenvalues, we have different zero-energy flows characterized by different wave numbers  $k = \sqrt{2M|E_r|}/\hbar$  corresponding to the negative-energy eigenvalues  $E_r < 0$ .

Provided that some external forces like electro-magnetic forces are put in the systems, the central motions possibly have potentials ( $V_C(\rho_C)$ ). In this case the zero-energy solutions appear when  $V_C(\rho_C)$  is written by one of the central potentials  $V_a(\rho_C)$ .

Here we note that in cases where the potentials of all the constituents have a negative constant potential  $V_0 < 0$  in a common area such as in the region surrounded by repulsive potentials like short distance attractive potentials as shown in fig. 1, the zero-energy solutions can appear in the area. In these cases we have to solve the zero-energy problems under some special boundary conditions. We will be able to find out the solutions fulfilling the boundary conditions in terms of the infinitely degenerate zero-energy solutions.

## (2) Velocity of the centre of mass system

It is obvious that we can introduce the velocity for the centre of mass system as same as that for the single particle given in section 2.1 such that

$$\mathbf{v}_C = \mathbf{j}_C(t, \vec{\rho}_C) / |\Phi_C(t, \vec{\rho}_C)|^2, \quad (11)$$

where the current for the centre of mass system is defined by  $\mathbf{j}_C(t, \vec{\rho}_C) = \text{Re}[\Phi_C^*(-i\hbar\nabla_{\rho_C})\Phi_C]/m$ . Since the derivative with respect to the centre of mass coordinate is just written by the sum of the derivatives of all the constituents, the velocity  $\mathbf{v}_C$  is understood as the mean velocity of the constituents. We may consider that  $\mathbf{v}_C$  represents the velocity that is used in hydrodynamics. Now it is trivial that in the case of the centre of mass motions we can follow the discussion on the vortices for the single particle motions presented in section 2.1.

We note that the velocity for a relative coordinate  $\rho_i$  can also be defined as same as that for the centre of mass coordinate such that

$$\mathbf{v}_i = \mathbf{j}_{\rho_i}/|\phi_r|^2, \quad (12)$$

where  $\mathbf{j}_{\rho_i} = \text{Re}[\phi_r^*(-i\hbar\nabla_{\rho_i})\phi_r]/m$ . We easily see that in independent particle models the above velocity coincides with that of the single particle given in section 2.1. If the central potentials of the type  $V_a(\rho)$  appear for some relative coordinates, the zero-energy flows appear, and then the zero-energy vortices are produced in the relative motions.

### 3. Vortex patterns in 2D-PPB

In order to see some concrete examples of stable and time-dependent vortex patterns we shall make some vortex patterns in terms of the eigenfunctions of the 2D-PPB [27]. As already noted, the stable patterns can be transformed to those of arbitrary potentials of the type  $V_a(\rho)$  by the conformal transformations [24,25].

#### 3.1 Eigenfunctions of 2D-PPB

Let us start from the short review on the eigenfunctions of the 2D-PPB  $V = -m\gamma^2(x^2 + y^2)/2$  that will be used in the following analyses. The infinitely degenerate eigenfunctions with the zero-energy for the potentials  $V_a(\rho)$  have explicitly been given in (5), whereas the eigenfunctions with non-zero energies are known only in the case of PPB [27-33]. It is trivial that the eigenfunctions in the 2D-PPB are represented by the multiples of those of the 1D-PPB. The eigenfunctions of the 1D-PPB for  $x$ , which have pure imaginary energy eigenvalues  $\mp i(n_x + \frac{1}{2})\hbar\gamma$ , are given by

$$u_{n_x}^{\pm}(x) = e^{\pm i\beta^2 x^2/2} H_{n_x}^{\pm}(\beta x) \quad (\beta \equiv \sqrt{m\gamma/\hbar}), \quad (13)$$

where  $H_{n_x}^{\pm}(\beta x)$  are the polynomials of degree  $n_x$  written in terms of Hermite polynomials  $H_n(\xi)$  with  $\xi = \beta x$  as [32, 33]

$$H_n^{\pm}(\xi) = e^{\pm i n \pi/4} H_n(e^{\mp i \pi/4} \xi). \quad (14)$$

We have four different types of the eigenfunctions in the 2D-PPB [27]. Two of them

$$U_{n_x n_y}^{\pm\pm}(x, y) \equiv u_{n_x}^{\pm}(x) u_{n_y}^{\pm}(y)$$

with the energy eigenvalues  $\mathcal{E}_{n_x n_y}^{\pm\pm} = \mp i(n_x + n_y + 1)$ , respectively, represent flows diverging from the origin and flows converging towards the origin. Some examples for the low degrees are obtained as follows;

$$\begin{aligned} U_{00}^{\pm\pm}(x, y) &= e^{\pm i\beta^2(x^2+y^2)/2}, \\ U_{10}^{\pm\pm}(x, y) &= 2\beta x e^{\pm i\beta^2(x^2+y^2)/2}, \\ U_{20}^{\pm\pm}(x, y) &= (4\beta^2 x^2 \mp 2i) e^{\pm i\beta^2(x^2+y^2)/2}, \\ U_{11}^{\pm\pm}(x, y) &= 4\beta^2 xy e^{\pm i\beta^2(x^2+y^2)/2}. \end{aligned} \quad (15)$$

Note that  $U_{01}^{\pm\pm}(x, y)$  and  $U_{02}^{\pm\pm}(x, y)$  are, respectively, obtained by exchanging  $x$  and  $y$  in  $U_{10}^{\pm\pm}(x, y)$  and  $U_{20}^{\pm\pm}(x, y)$ . It is transparent that the eigenfunctions of angular momentums are constructed in terms of the linear combinations of these diverging and converging flows [27]. The other two

$$U_{n_x n_y}^{\pm\mp}(x, y) \equiv u_{n_x}^{\pm}(x)u_{n_y}^{\mp}(y) \quad \text{with} \quad \mathcal{E}_{n_x n_y}^{\pm\mp}(x, y) = \mp i(n_x - n_y)$$

are corner flows round the center. (See figs. 2 and 3.) The zero-energy solutions that are common in the potentials  $V_a(\rho)$  appear when  $n_x = n_y$  is satisfied. A few examples of the zero-energy eigenfunctions are explicitly obtained as follows;

$$\begin{aligned} U_{00}^{\pm\mp}(x, y) &= e^{\pm i\beta^2(x^2 - y^2)/2}, \\ U_{11}^{\pm\mp}(x, y) &= 4\beta^2 xy e^{\pm i\beta^2(x^2 - y^2)/2}, \\ U_{22}^{\pm\mp}(x, y) &= 4[4\beta^4 x^2 y^2 + 1 \pm 2i\beta^2(x^2 - y^2)]e^{\pm i\beta^2(x^2 - y^2)/2}. \end{aligned} \quad (16)$$

It is obvious that the eigenfunctions of (15) and (16) are not normalizable. The proof that they are the eigenfunctions of CSGT are presented in refs. [32,33].

### 3.2 Stable vortex-patterns

Let us investigate vortex patterns in terms of the 2D-PPB eigenfunctions. Since the zero-energy solution given in the section 3.1 have no nodal point with non-vanishing currents, they have no vortex. However, it has been shown that some vortex patterns having infinite numbers of vortices, like vortex lines and vortex lattices, can be made in terms of simple linear combinations of those low lying stationary states in the early works [24, 25]. We shall here study linear combinations having a few or some vortices observed in experiments [6-14]. Let us start from compositions of stable vortex patterns. For the convenience in the following discussions we take the flow without any vortices described by

$$\begin{aligned} \Phi_B &= \frac{1}{4}U_{22}^{+-}(x, y) - U_{00}^{+-}(x, y) \\ &= (4\beta^4 x^2 y^2 + 2i\beta^2(x^2 - y^2))e^{i\beta^2(x^2 - y^2)/2}, \end{aligned} \quad (17)$$

which will be called the basic flow hereafter. Note that the nodal point of the basic flow at the origin does not produce vortices, because the current vanishes there.

Here we shall show three stable patterns, which will be used in the discussions on vortex creations and annihilations.

#### (S-1) Three-vortices pattern

The linear combination of the basic flow and  $U_{11}^{+-}$  such that

$$\begin{aligned} \Phi_{012}^{+-}(x, y) &= \Phi_B - c^2 U_{11}^{+-}(x, y) \\ &= [4\beta^2 xy(\beta^2 xy - c^2) + 2i\beta^2(x^2 - y^2)]e^{i\beta^2(x^2 - y^2)/2}, \end{aligned} \quad (18)$$



with  $c \in \mathbb{R}$  has three vortices at the origin and the two points  $(\pm c/\beta, \pm c/\beta)$  as shown in fig. 4. If we take  $-c^2$  instead of  $c^2$ , three vortices appear at the origin and the points  $(\pm c/\beta, \mp c/\beta)$ .

### (S-2) One-vortex pattern

Let us consider the linear combinations of two flows that are represented by the above eigenfunction  $\Phi_{012}^{+-}(x, y)$  and coming from two different directions such that

$$\Phi_{012}^{+-}(x, y) + \Phi_{012}^{+-}(\xi, \eta), \quad (19)$$

where  $\xi = \cos\alpha \cdot x + \sin\alpha \cdot y$  and  $\eta = -\sin\alpha \cdot x + \cos\alpha \cdot y$  with  $0 < \alpha < 2\pi$ . It is apparent that the two functions have only one common zero-point at the origin for  $0 < \alpha < 2\pi$ . We see that the vortex at the origin has the circulation number  $l = -2$ .

### (S-3) Four-vortices pattern

The linear combinations given by

$$\begin{aligned} \Phi_{02}^{+-}(x, y) &= \frac{1}{4}\Phi_B - c^4 U_{00}^{+-}(x, y) \\ &= [(\beta^2 xy - c^2)(\beta^2 xy + c^2) + i\beta^2(x^2 - y^2)/2]e^{i\beta^2(x^2 - y^2)/2}, \end{aligned} \quad (20)$$

has four vortices at the points  $(\pm c/\beta, \pm c/\beta)$  and  $(\pm c/\beta, \mp c/\beta)$  as shown in fig. 5.

## 3.3 Moving vortex-patterns

Let us go to the study of time-dependent vortex patterns, where vortices can move, and sometimes be created and annihilated. Such patterns are obtained by linear combinations of stable flows and time-dependent ones. In the following considerations the time dependent flows are put in the stable flows at  $t = 0$ .

### (M-1) A pattern accompanied by a pair creation and annihilation

Let us consider the following linear combination;

$$\begin{aligned} \Phi_{02,1}^{+-}(x, y, t) &= \frac{1}{2}\Phi_B - \theta(t)c^3 U_{10}^{+-}(x, y)e^{-\gamma t} \\ &= [2\beta x(\beta^3 xy^2 - \theta(t)c^3 e^{-\gamma t}) + i\beta^2(x^2 - y^2)]e^{i\beta^2(x^2 - y^2)/2}, \end{aligned} \quad (21)$$

where the theta function is taken as  $\theta(t) = 0$  for  $t < 0$  and  $= 1$  for  $t \geq 0$ . It has two nodal points at  $(ce^{-\gamma t/3}/\beta, \pm ce^{-\gamma t/3}/\beta)$  for  $t \geq 0$ , where two vortices with opposite circulation numbers exist. The nodal points go to the origin as the time  $t$  goes to infinity as shown in fig. 6. Since the contribution of the unstable flow decreases as  $t \rightarrow \infty$  because of the time factor  $e^{-\gamma t}$ , the wavefunction  $\Phi_{02,1}^{+-}(x, y, t)$  goes to  $\Phi_B/2$  as  $t \rightarrow \infty$ . Thus the flow has no nodal point in the limit. This means that the pair of vortices which are created at  $t = 0$  disappears at origin in the limit  $t \rightarrow \infty$ . We can say that this wavefunction describes the pair annihilation of two vortices. The time development of this process can be described as follows:

- (i) Before the time-dependent flow is put in the basic flow, i.e.,  $t < 0$ , there is no vortex.
- (ii) At  $t = 0$  when the time-dependent flow is put in the basic flow, a pair of vortices are

suddenly created.

(iii) The pair moves toward the origin, and then they annihilate at the origin, that is, the flow turns back to the basic flow  $\Phi_B$  having no vortex.

**(M-2) A pattern accompanied by creations and annihilations of two pairs**

The linear combination given by

$$\begin{aligned}\Phi_{02,2}^{+-}(x, y, t) &= \Phi_B - \theta(t)c^2[2iU_{00}^{+-}(x, y) - U_{20}^{+-}(x, y)e^{-2\gamma t}] \\ &= [4\beta^2x^2(\beta^2y^2 - \theta(t)c^2e^{-2\gamma t}) - 2i(\theta(t)c^2(1 - e^{-2\gamma t}) - \beta^2(x^2 - y^2))]e^{i\beta^2(x^2 - y^2)/2}\end{aligned}\quad (22)$$

has four nodal points at  $(\pm c/\beta, ce^{-\gamma t}/\beta)$  and  $(\pm c/\beta, -ce^{-\gamma t}/\beta)$  for  $t \geq 0$ . In this case we easily see that the pair of vortices at  $(\pm c/\beta, ce^{-\gamma t}/\beta)$  and that at  $(\pm c/\beta, -ce^{-\gamma t}/\beta)$  annihilate as  $t \rightarrow \infty$  as shown in fig. 7. The stable flow  $\Phi_B - 2ic^2U_{00}^{+-}(x, y)$  that appears in the limit has two nodal points at  $(\pm c/\beta, 0)$ , but it has no vortex but two vortex dipoles, because the current also vanishes at the points. The time development of this process is interpreted similarly as the case (M-1).

In these two cases all vortices move on straight lines in the pair annihilation processes.

**(M-3) A pattern accompanied by creation and annihilation of four vortices**

The linear combinations of stationary flows and diverging or converging ones make different types of annihilation processes. For an example, let us consider the linear combination of  $\Phi_B$  and the lowest order diverging flow described by

$$U_{00}^{++}(x, y, t) = e^{i\beta^2(x^2 + y^2)/2}e^{-\gamma t} \quad (23)$$

having the energy eigenvalue  $-i\gamma\hbar$ . Let us consider the linear combination described by

$$\begin{aligned}\Phi_{02,0}^{++}(x, y, t) &= \frac{1}{4}\Phi_B - \theta(t)c^2U_{00}^{++}(x, y, t) \\ &= [\beta^4x^2y^2 - \theta(t)c^2e^{-\gamma t}e^{i\beta^2y^2} + i\beta^2(x^2 - y^2)/2]e^{i\beta^2(x^2 - y^2)/2}.\end{aligned}\quad (24)$$

For  $t \geq 0$  it has two nodal points at the points where the following relations are fulfilled;

$$XY = c(t)\cos Y, \quad \frac{1}{2}(X - Y) - c(t)\sin Y = 0, \quad (25)$$

where  $X = \beta^2x^2$ ,  $Y = \beta^2y^2$  and  $c(t) = c^2e^{-\gamma t}$ . From these relations we have an equation for  $Y$

$$Y^2 - c(t)\cos Y + 2c(t)Y\sin Y = 0. \quad (26)$$

The solutions are obtained from the cross points of two functions  $f(Y) = Y^2$  and  $g(Y) = c(t)(\cos Y - 2Y\sin Y)$ . We easily see that a solution for  $Y \geq 0$  exists in the region  $0 < Y < \pi/2$  for arbitrary positive numbers of  $c(t)$ . Four vortices appear at the four points expressed by the combinations of  $x = \pm\sqrt{X}/\beta$  and  $y = \pm\sqrt{Y}/\beta$ , where  $X$  is obtained by using the first relation of (25). Since  $c(t)$  goes to 0 as  $t \rightarrow \infty$ , we see that  $X$  and  $Y$  simultaneously go to 0 in the limit such that

$$X \simeq Y \rightarrow |c|e^{-\gamma t/2} \rightarrow 0, \quad \text{for } t \rightarrow \infty.$$

Since the flow turns back to the basic flow, the four vortices annihilate at the origin in the limit. From the second relation of (25), we have

$$X = Y + 2c(t)\sin Y.$$

This equation show us that the vortex points do not move along straight lines.

Here we consider a somewhat complicated processe.

**(M-4) A pattern accompanied by annihilation of four vortex-pairs**

Here we take  $\Phi_{02}^{+-}(x, y)$  of (20) as the stable flow, which has four vortices. For the simplicity  $c = 1/2$  is taken in the following discussions. Here the lowest order diverging flow  $U_{00}^{++}(x, y, t)$  are put into the stationary flow at  $t = 0$ . The wavefunction are given by

$$\begin{aligned} \Phi_{02,0}^{++}(x, y; t) &= 16\Phi_{02}^{+-}(x, y) + \theta(t)b^2U_{00}^{++}(x, y, t) \\ &= [16\beta^4x^2y^2 - 1 + \theta(t)b^2e^{-\gamma t}e^{i\beta^2y^2} + 8i\beta^2(x^2 - y^2)]e^{i\beta^2(x^2 - y^2)/2} \\ &= [16\beta^4x^2y^2 - 1 + \theta(t)b(t)e^{-\gamma t}\cos(\beta^2y^2) + i(8\beta^2(x^2 - y^2) \\ &\quad + \theta(t)b(t)e^{-\gamma t}\sin(\beta^2y^2))]e^{i\beta^2(x^2 - y^2)/2}, \end{aligned} \quad (27)$$

where  $b \in \mathbb{R}$  and  $b(t) = b^2e^{-\gamma t}$ . Using  $X = \beta^2x^2$  and  $Y = \beta^2y^2$ , we have two relations for nodal points of the wavefunction for  $t > 0$  as follows;

$$16XY + b(t)\cos Y - 1 = 0, \quad 8(X - Y) + b(t)\sin Y = 0. \quad (28)$$

From these relations we obtain an equation for the nodal points

$$1 - b(t)\cos Y - 16Y^2 + 2b(t)Y\sin Y = 0. \quad (29)$$

Examining the cross point of the two functions  $F(Y) = 16Y^2 - 1$  and  $G(Y) = -b(t)(\cos Y - 2Y\sin Y)$ , we obtain the following results:

(1) In the case of  $b(t) < 1$  the two functions always have a cross-point in the region satisfying  $Y \geq 0$  (note that  $Y = \beta^2y^2$ ). The wavefunction, therefore, has four nodal points. This means that the flow always has four vortices that move toward the stationary points fulfilling  $|x| = |y| = (2\beta)^{-1}$  as  $t$  increases.

(2) In the case of  $b(t) > 1$ , eq.(29) has an even number of solutions like  $n = 0, 2, 4, \dots$ . Since one solution brings four vortices on a circle with the centre at the origin, the vortex number is given by  $4n$ . Note that the number  $n$  increases as  $b(t)$  increases. This fact means that, since  $b(t)$  decreases as  $t$  increases, the vortex number decreases as  $t$  increases, until  $b(t)$  gets to 1. Considering that the change of  $n$  is always 2, we see that the reduction of the vortex number caused by the change of  $n$  is always 8. That is to say, we observe that four vortex-pairs simultaneously annihilate at four different points on a circle. As a simple example, let us consider the case of  $n = 2$  at  $t = 0$ . We observe the following time development of the flow:

(i) For  $t < 0$  the stationary flow has the four vortices as shown in fig.5.

(ii) At  $t = 0$  the original four vortices are disappear and eight vortices are newly created.

Then we observe the flow having eight vortices. (See fig. 8.)

(iii) In the time-evolution the eight vortices disappear simultaneously. We observe the process as the annihilations of four vortex-pairs. Thus the flow having no vortex appears.

(iv) At the critical time  $t_c = \ln b^2 / \gamma$  when  $b(t_c) = 1$  is fulfilled four vortices are created at the origin, and then they move toward the stationary points. The vortex state at  $t = t_c$  can be understood as a vortex quadrupole [24].

If, instead of the diverging flow  $U_{00}^{++}(x, y, t)$ , the converging flow  $U_{00}^{--}(x, y, t)$  is put in the stationary flow, we observe a flow continuously creating 8 vortices for any choices of  $b$ . Of course, the time dependent flow blows up the magnitude in the limit of  $t \rightarrow \infty$ , and thus the original stable flow can not be observed in the limit.

#### 4. Interesting properties of zero-energy flows

Let us here consider interesting properties of the zero-energy flows. The first interesting property is due to the fact that the use of the zero-energy flows is very useful and economical from the viewpoint of energy consumption. For example it can be a very economical step for the transmission of information. Considering the huge variety arising from the infinite degeneracy, the transmission by the use of the zero-energy flows enable us to transmit an enormous amount of information without any energy loss. The flows are stable and then they can also be a very useful step for making mechanisms to preserve such information, e.g., for memories in living beings. The huge variety of vortex patterns can possibly discriminate the enormous amount of information. The addition of new memories and also the change of preserved memories can easily be carried out by pouring some zero-energy (stable) flows in the preserved ones. Furthermore, as shown in section 3.3, in all the time-dependent processes induced by pouring the unstable flows with complex energy eigenvalues the time-dependent flows always turn back to the stable flows in the long time scales, and then the initial flow patterns are recovered. That is to say, the initial patterns are kept in all such time-dependent processes. This stability of the flow patterns seems to be a very interesting property for the interpretation of the stability of memories not only in their preservations but in their applications as well. The applications, of course, mean thinking processes. These flows will possibly be workable in the steps for thinking in living beings. The use of the zero-energy and complex-energy solutions enables living beings to make up many functions in their bodies very economically on the basis of energy consumption. Anyway the zero-energy and complex-energy solutions are interesting objects to describe mechanisms working very economically as for the energy consumption. Especially, in the 2D-PPB case we can do it without any energy loss, because all the solutions of PPB have no real energy eigenvalue, i.e., the energy eigenvalues are zero or pure imaginary.

Here we would like to summarize the property of flows in CSGT. As for the zero-energy flows we can stress the following three properties; they can be

- (i) the absolutely energy-saving mechanism,
- (ii) the mechanism including an enormous topological variety in terms of vortex patterns, and also

(iii) the perfect mechanism to recover the initial flow patterns in any disturbance by pouring arbitrary decaying flows with complex-energy eigenvalues.

The role of the flows with complex energies will be understood as short excitement mechanisms of the vortex patterns. We still have a lot of problems to overcome the present situation, but we may expect that the study of the zero- and complex-energy solutions in CSGT will open a new site in physics.

## 5. Remarks

We have shown concrete examples of different types of vortex patterns accompanied by creations and annihilations of vortices by using only some low degree solutions of the 2D-PPB. We can, of course, present more complicated patterns by introducing the higher degree solutions, but the examples presented in the sections 3 will be enough to show the fact that various vortex patterns can be reproducible in terms of the eigenfunctions of the 2D-PPB. As already noted that the zero-energy solutions in the 2D-PPB can be transformed to those in the potentials  $V_a(\rho)$  by the conformal transformations [24,25], the stable patterns given in section 3.2 can be transformed into the stable patterns of arbitrary potentials. This fact means that, as far as the stable patterns are concerned, there is an exact one-to-one correspondence between the patterns of the PPB and those of the other potentials. As for the time-dependent patterns we cannot present any concrete examples except the case of the 2D-PPB at this moment, but we may expect that similar vortex patterns as those given in section 3.3 for the PPB will appear in other potentials, since all energy eigenstates with complex eigenvalues degenerate infinitely in all the potentials  $V_a(\rho)$  as same as in the 2D-PPB. Anyhow we cannot exactly say about the problem before we find any solutions with complex eigenvalues in the other cases.

Here we would like to note 2D-PPB. We do not know any physical phenomena that are described by 2D-PPB. We can, however, expect that most of weak repulsive forces in matters composed of many constituents will be approximated by PPBs as most of weak attractive forces are well approximated by harmonic oscillators. In general flows that go round a smooth hill of potential feel a weak repulsive force represented by a PPB [34-36]. Actually we see that when a charged particle is put in an infinitely long tube where same charged particles are uniformly distributed, the charged particle feels 2D-PPB. In non-neutral plasma electrons being near the center will possibly be in a similar situation. In the plasma electro-magnetic interactions must be introduced. It should be noted that in the case of a charged particle in a magnetic field the vortex quantization given by (6) can be read as

$$\begin{aligned} m\Gamma &= \oint_c (\nabla S - q\mathbf{A}) \cdot d\mathbf{s} \\ &= \oint_c \mathbf{p} \cdot d\mathbf{s} - q\Phi, \end{aligned} \tag{30}$$

where  $q$  is the charge of the particle and  $\Phi$  is the magnetic flux passing through the enclosed surface. Analyzing vortex phenomena of non-neutral plasma in terms of the

eigenfunctions of the 2D-PPB will be an interesting application.

The infinite freedom arising from the infinite degeneracy of the zero-energy solutions should be noticed. Such a freedom has never appeared in the statistical mechanics describing thermal equilibrium. The freedom is different from that generating the usual entropy and then temperatures, because the freedom does not change real energy observed in experiments at all. A model of statistical mechanics for the new freedom has been proposed and some simple applications have been performed in the case of 1D-PBB [37-39]. The model is applicable to slowly changing phenomena in the time evolutions, because the PPB has only pure imaginary energy eigenvalues in the 1-dimension. In the present model of the 2-dimensions, however, we have the infinite degree of freedom arising from the zero-energy solutions that have no time evolution. The huge degeneracy of the zero-energy solutions can provide the huge variety in every energy eigenstate, which will be identified by the vortex patterns. In such a consideration the vortex patterns will be understood as the topological properties of flows. How this freedom should be counted in statistical mechanics is an important problem in future considerations.

Finally we would like to comment on the meaning of the eigenstates in CSGT. As already noted, the eigenfunctions in CSGT are generally not normalizable, and then the probability and the probability current cannot have a definite meaning. This fact means that the probabilistic interpretation for the eigenfunctions cannot be introduced in CSGT. How should we interpret the eigenfunctions in CSGT? From the discussions presented in this paper we find out a possible idea that the quantization in terms of Gel'fand triplets describes the quantization of flows. Flows are, of course, composed of many particles, and then the probability used in the description of one particle motions cannot be introduced. The magnitudes of the eigenfunctions should be considered to be proportional to the densities of the flows like the intensity of beams in scattering processes. Thus the normalizations of wavefunctions expressed by the linear combinations of the eigenfunctions lose the meaning in CSGT. We can, however, find out that the energies are quantized as discrete or continuous numbers including complex numbers, and also the flows expressed by the eigenfunctions interfere. Though quantities in CSGT are in general not directly observed except eigenvalues such as energies, we see that velocities have a special role that they are observables being definable only on CSGT. Vortex patterns that are determined only from nodal points of wavefunctions are also good observables to investigate solutions in CSGT. As shown in section 3, we can actually see the interferences among flows through the investigation of the vortex patterns. We may say that hydrodynamical approach will be an interesting trial to investigate physics in CSGT.

## References

- [1] G. Blatter *et al.*, Rev. Mod. Phys. **66**, 1125 (1994).
- [2] G. W. Crabtree and D. R. Nelson, Phys. Today **50**, No.4 38 (1997).
- [3] R. E. Prange and M. Girvin M, *The Quantum Hall Effect* (Springer, New York, 1990), 2nd ed.
- [4] T. Chakaraborty and P. Pietiläinen, *The Quantum Hall Effects: Fractional and Integral* (Springer, New York, 1995), 2nd and updated ed.
- [5] S. Das Sarma and A. Pinczuk, A eds 1997 *Perspectives in Quantum Hall Effects* (Wiley, New York, 1997).
- [6] K. S. Fine *et al.*, Phys. Rev. Lett. **75**, 3277 (1995).
- [7] Y. Kiwamoto *et al.*, J. Phys. Soc. Jpn. (Lett.) **68**, 3766 (1999).
- [8] Y. Kiwamoto *et al.*, Phys. Rev. Lett. **85**, 3173 (2000).
- [9] K. Ito *et al.*, Jpn. J. Appl. Phys. **40A**, 2558 (2001).
- [10] M. R. Matthews *et al.*, Phys. Rev. Lett. **83**, 2498 (1999).
- [11] C. Raman *et al.*, Phys. Rev. Lett. **83**, 2502 (1999).
- [12] K. W. Madison *et al.*, Phys. Rev. Lett. **84**, 806 (2000).
- [13] O. M. Marago *et al.*, Phys. Rev. Lett. **84**, 2056 (2000).
- [14] R. Fitzgerald *et al.*, Phys. Today **55**, No.8 19 (2000).
- [15] J. O. Hirschfelder, A. C. Christoph and W. E. Palke, J. Chem. Phys. **61**, 5435 (1974).
- [16] J. O. Hirschfelder, C. J. Goebel and L. W. Bruch, J. Chem. Phys. **61**, 5456 (1974).
- [17] J. O. Hirschfelder and K. T. Tang, J. Chem. Phys. **64**, 760; *ibid.* **65**, 470 (1976).
- [18] J. O. Hirschfelder, J. Chem. Phys. **67**, 5477 (1977).
- [19] S. K. Ghosh and B. M. Deb, Phys. Rep. **92**, 1 (1982).
- [20] H. Wu and D. W. L. Sprung, *Phys. Letters A* **183**, 413 (1993).
- [21] J. C. Ryan and A. K. Rajagopal, *Phys. Rev.* **B47**, 8843 (1993).
- [22] D. A. Schecter and H. E. Dubin, *Phys. Rev. Lett.* **83**, 2191 (1999).

- [23] I. Bialynicki-Birula, Z. Bialynicka-Birula and Śliwa C, *Phys. Rev.* **A61**, 032110 (2000).
- [24] T. Kobayashi, *Physica* **A303** (2002) 469 .
- [25] T. Kobayashi and T. Shimbori, *Phys. Rev.* **A65**, 042108 (2002).
- [26] A. Bohm and M. Gadella, *Dirac Kets, Gamow Vectors and Gelfand Triplets* (Lecture Notes in Physics, Vol. 348, Springer, 1989).
- [27] T. Shimbori and T. Kobayashi, *J. Phys.* **A33**, 7637 (2000).
- [28] G. Barton, *Ann. Phys. (N.Y.)* **166**, 322 (1986).
- [29] P. Briet, J. M. Combes and P. Duclos, *Commun. Partial Diff. Eqns.* **12**, 201 (1987).
- [30] N. L. Balazs and A. Voros, *Ann. Phys. (N.Y.)* **199**, 123 (1990).
- [31] M. Castagnino, R. Diener, L. Lara and G. Puccini, *Int. J. Theor. Phys.* **36**, 2349 (1997).
- [32] T. Shimbori and T. Kobayashi, *Nuovo Cimento Soc. Ital. Fis., B* **115**, 325 (2000).
- [33] T. Shimbori, *Phys. Lett. A* **273**, 37 (2000).
- [34] M. S. Child, *Proc. Roy. Soc. (London)* **A292** (1966) 272.
- [35] M. S. Child, *Mol. Phys.* **12** (1967) 401.
- [36] J. N. L. Connor, *Mol. Phys.* **15** (1968) 37.
- [37] T. Kobayashi and T. Shimbori, Statistical mechanics for states with complex eigenvalues and quasi-stable semiclassical systems *Preprint cond-mat/0005237* (2000).
- [38] T. Kobayashi and T. Shimbori, *Phys. Lett.* **A280**, 23 (2001).
- [39] T. Kobayashi and T. Shimbori, *Phys. Rev.* **E63**, 056101 (2001).



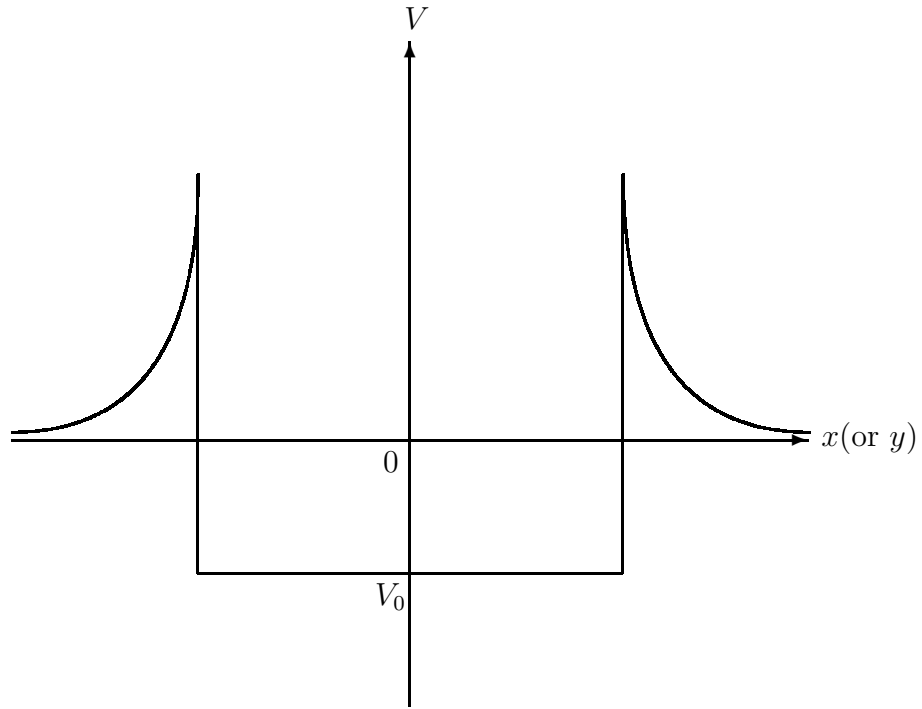


FIG. 1: An example of the potentials with zero-energy solutions.

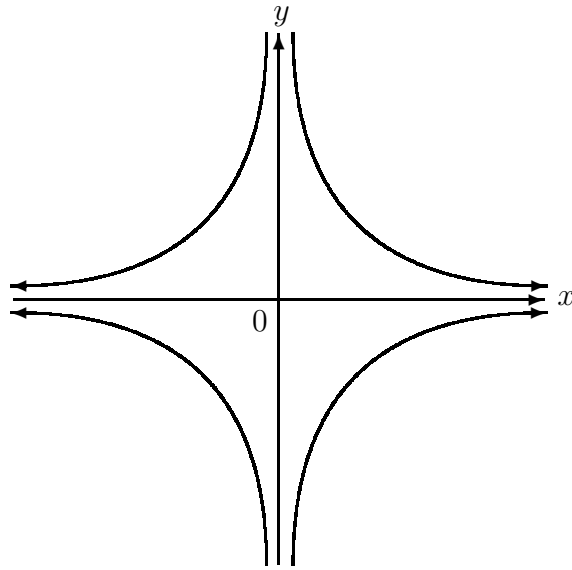


FIG. 2: Corner flows moving from the  $y$ -direction to the  $x$ -direction.

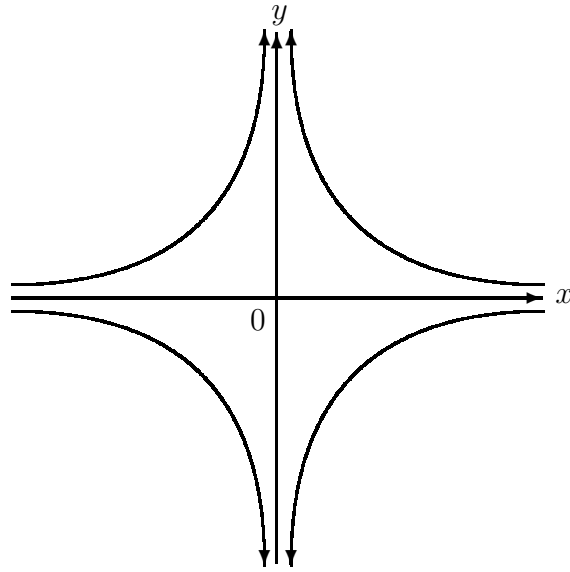


FIG. 3: Corner flows moving from the  $x$ -direction to the  $y$ -direction.

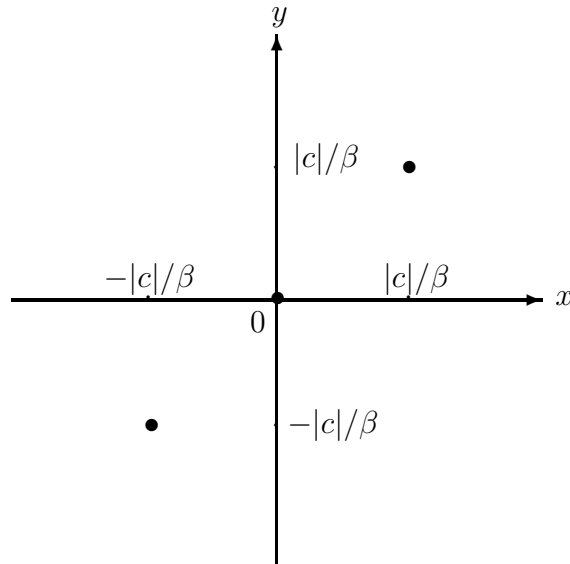


FIG. 4: Stationary pattern with three vortices.  $\bullet$  denotes a vortex.

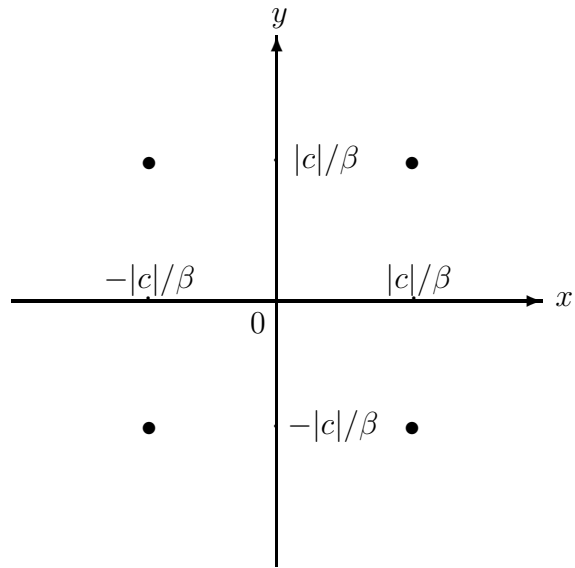


FIG. 5: Stationary pattern with four vortices.

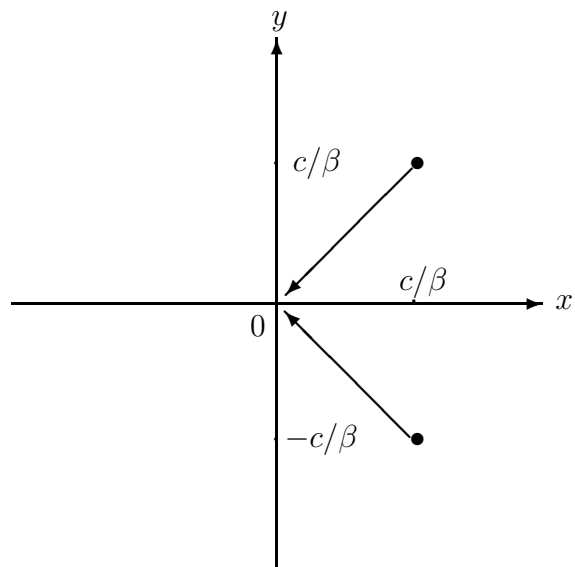


FIG. 6: A pair annihilation pattern for  $c > 0$ . The arrows show the moving directions of the vortices.

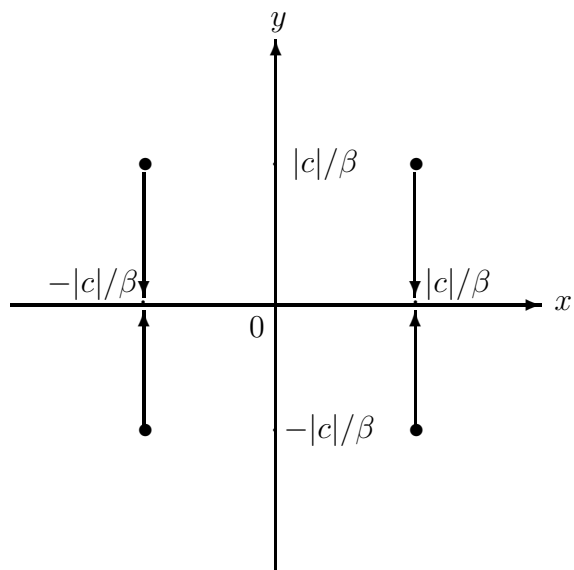


FIG. 7: Two pairs annihilation pattern.

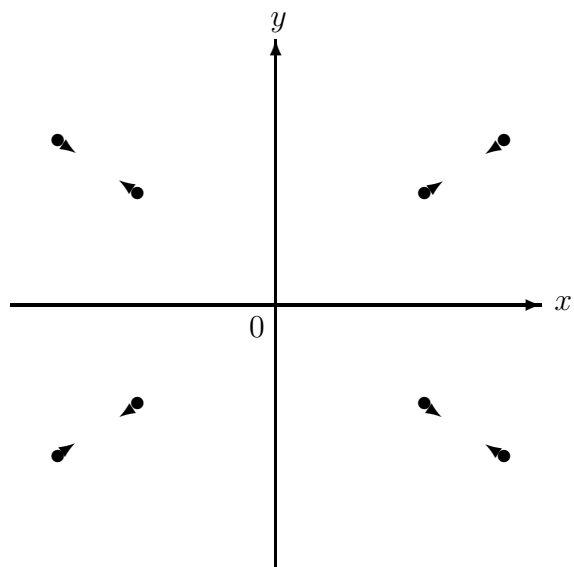


FIG. 8: Four pairs creation and annihilation.